ORIGINAL PAPER

Surface Modification of Poly-ε-Caprolactone with an Atmospheric Pressure Plasma Jet

N. De Geyter · A. Sarani · T. Jacobs · A. Yu. Nikiforov · T. Desmet · P. Dubruel

Abstract In this work, poly-ε-caprolactone samples are modified by an atmospheric pressure plasma jet in pure argon and argon/water vapour mixtures. In a first part of the paper, the chemical species present in the plasma jet are identified by optical emission spectroscopy and it was found that plasmas generated in argon/0.05 % water vapour mixtures show the highest emission intensity of OH (A–X) at 308 nm. In a subsequent section, plasma jet surface treatments in argon and argon/water vapour mixtures have been investigated using contact angle measurements and X-ray photoelectron spectroscopy. The polymer samples modified with the plasma jet show a significant decrease in water contact angle due to the incorporation of oxygen-containing groups, such as C–O, C=O and O–C=O. The most efficient oxygen inclusion was however found when 0.05 % of water vapour is added to the argon feeding gas, which correlates with the highest intensity of OH (X) radicals. By optimizing the OH (X) radical yield in the plasma jet, the highest polymer modification efficiency can thus be obtained.

Introduction

Tissue engineering is a new and exciting research field aiming to construct living structures that restore, maintain or improve diseased tissues or organs functions [1, 2]. One of the main current approaches involves the culturing of cells in (bio)degradable three-dimensional artificial matrices (so-called scaffolds), which offer optimal support and conditions

N. De Geyter (✉) · A. Sarani · T. Jacobs · A. Yu. Nikiforov
Research Unit Plasma Technology (RUPT), Department of Applied Physics, Faculty of Engineering and Architecture, Ghent University, Sint-Pietersnieuwstraat 41, 9000 Ghent, Belgium
e-mail: Nathalie.DeGeyter@Ugent.be

T. Desmet · P. Dubruel
Polymer Chemistry and Biomaterials Group, Department of Organic Chemistry, Faculty of Sciences, Ghent University, Krijgslaan 281 S4, 9000 Ghent, Belgium

for tissue growth [3, 4]. Ideally, scaffolds should meet several design criteria. The materials should: (1) possess mechanical properties matching those of the tissue to be replaced, (2) be reproducibly processable into three-dimensional porous scaffolds, (3) be biocompatible and if required biodegradable and (4) possess surface properties enabling cell adhesion, proliferation and differentiation [5–8].

Biodegradable, aliphatic polyesters have been extensively studied as scaffold materials since they possess good mechanical and biocompatible properties as well as adjustable degradation rates depending on the selected polymer [9]. However, the hydrophobicity and low surface energy of these polyesters lead to low cell attachment, spreading and proliferation [10]. To overcome this limitation, surface modification can be applied. Several approaches have been developed with this aim. A commonly used strategy is to chemically modify the polyesters by introducing specific functional groups on the surface [11, 12]. Although these wet-chemical processes are very useful, some drawbacks should be noted. Some of these modification techniques can be quite harsh and can thus result in certain undesirable effects such as a loss of mechanical properties and a faster degradation process [4, 13]. In addition, these chemical methods generate hazardous chemical waste. Alternatively, reactive functional groups can be introduced by peroxide oxidation, ozone oxidation and γ-and UV-radiation, however, these techniques also involve degradation of the polymers and usually result in non-permanent effects [14–16]. In contrast to the previously described surface modification techniques, plasma treatment is a very convenient strategy. This technique can efficiently incorporate functional groups on the surface of biodegradable polyesters without changing the beneficial bulk properties [17]. Moreover, it can be employed to uniformly treat the surface of complex shaped scaffolds [9]. In addition, the use of hazardous solvents can be avoided as plasma treatment is a solvent-free technique [4]. Because of these numerous advantages, plasma surface modification of biodegradable polyesters demonstrates great potential.

The work in the present paper will specifically focus on plasma modification of poly-ε-caprolactone (PCL), a commonly used biodegradable, aliphatic polyester, with a chemical structure shown in Fig. 1. A few authors have already studied the effect of non-thermal plasmas on PCL samples, however, their studies mostly focus on low pressure plasma technologies [8, 13, 18]. Although these low pressure plasma treatments afford good control over gas chemistry and enable the application of high energetic species, atmospheric pressure plasma technologies offer attractive perspectives in today's industrial processes due to the elimination of expensive vacuum equipment, easier handling of the samples and scalability for in-line processing [19, 20]. Therefore, in recent years, a lot of effort has been invested into the development of non-thermal plasma reactors working at atmospheric pressure [20, 21]. Recently, there have been some studies on the surface modification of PCL using atmospheric pressure plasmas such as DBDs [22–24] and RF plasmas [25, 26]. However, an atmospheric pressure plasma jet (APPJ) has not yet been applied for the surface modification of PCL despite its numerous benefits. This discharge is easy to integrate into existing production lines and can selectively treat specific parts of a substrate [27–29]. Moreover, in contrast to most corona and dielectric barrier discharges, APPJs are not limited to flat and thin substrates, but can also be used to modify large three-dimensional structures [27, 30].

Fig. 1 Chemical structure of poly-ε-caprolactone (PCL)

$$\left[(CH_2)_5 - \overset{\overset{\displaystyle O}{\|}}{C} - O \right]_n$$
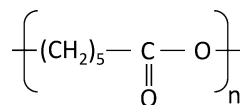
Taking into account these advantages, an APPJ will be used in this work for the surface modification of PCL. After the description of the experimental procedures, the optical characteristics of the plasma jet will be discussed for different working gases (argon and argon/water vapour mixtures). In a subsequent section, plasma jet surface treatments in argon and argon/water vapour mixtures will be investigated. The influence of different plasma operating parameters on PCL surface properties will be explored in detail using contact angle measurements (for wettability determination) and X-ray photoelectron spectroscopy (XPS, for chemical composition determination).

Experimental Procedure

PCL Samples

To optimize the plasma modification parameters, the present study focuses on flat non-porous PCL substrates. The flat PCL samples (20 mm × 20 mm) are produced from PCL granules with a weight average molecular weight M_w of 80.000 g/mol (Sigma-Aldrich, Belgium). 1.5 grams of these granules are placed in moulds, which are subsequently heated in a vacuum oven at 120 °C for 1 h. Afterwards, the moulds are allowed to cool down to room temperature overnight before removing the samples by dissembling the moulds. Prior to plasma treatment, the PCL samples are rinsed once in Disinfectol® for 3 min.

Atmospheric Pressure Plasma Jet (APPJ) Set-up and Characterization

A schematic representation of the used experimental set-up is shown in Fig. 2, together with an image of the plasma jet in pure argon. The discharge is generated inside a quartz capillary with inside and outside diameters of 1.3 and 3.0 mm, respectively. The high-voltage electrode is a tungsten wire (diameter = 0.5 mm) with a half-sphere-shaped tip. The second ring-shaped ground electrode (length = 10 mm) is placed outside the capillary at a distance of 10 mm from the high-voltage electrode and 10 mm away from the edge of the capillary. PCL samples are modified by the plasma jet by scanning the polymer surface with adjustable scanning velocities (0.1–5.0 m/min). High purity argon is used for plasma generation with flow rates ranging between 0.5 and 3.0 standard litres per minute (slm). Water vapour can be introduced to the argon plasma jet via a bubbling system containing distilled water, carried by a secondary argon flow. By changing the argon gas flow through the bubbling system, the water content in the argon/water vapour plasma jet can be varied between 0.0 and 0.5 %. The water vapour percentage is calculated using the following equation:

$$\% \, H_2O = 100 \frac{P_{H_2O}}{P_{H_2O} + P_{gas}}$$

where P_{gas} is the gas pressure (101,325 Pa) and P_{H_2O} the water vapour pressure. According to Hibert et al. [31], this water vapour pressure is determined by the pure argon gas flow rate (F_1) and the flow rate of gas saturated with water vapour after bubbling (F_2):

$$P_{H_2O}[Pa] = 2338 \frac{F_2}{F_1 + F_2}$$

The jet is generated by applying an AC voltage (fixed frequency = 50 kHz) to the high-voltage electrode with peak-to-peak values ranging from 6 to 12 kV. At an applied voltage

of less than 6 kV (peak-to-peak), only a weak radiation zone is observed inside the capillary on the tip of the high-voltage electrode, which is a well-known corona discharge. However, an increase in the applied voltage results in the formation of a bright plasma in the inter-electrode gap with a long outflowing plasma propagating in the surrounding air, as shown in Fig. 2. The voltage applied to the high-voltage electrode is measured using a high voltage probe (Tektronix P6015A), whereas a current transformer (Ion Physics CM-100L) is used to measure the discharge current. The voltage-current waveforms are then recorded using a Tektronix TDS 1002 digital oscilloscope. Using these voltage-current waveforms, the average power W of the discharge is calculated according to the following equation (T = period of the discharge) [32]:

$$W = \frac{1}{T} \int\limits_{t}^{t+T} I(t)V(t)dt \qquad (1)$$

To identify the reactive species generated in the discharge, optical emission spectra are recorded by means of an Ocean Optic S2000 spectrometer in the range 250–900 nm with a resolution of 0.7 nm. These spectra are obtained 4 mm from the edge of the capillary: this allows us to determine which plasma species interact with the polymer surface, since most surface modifications in this work are performed on PCL samples placed 4 mm from the edge of the capillary. Optical emission spectra at different distances from the edge of the capillary have already been performed by Nikiforov et al. [33] and will therefore not be presented in this work.

Water Contact Angle Measurements

The wettability of the PCL samples, determined a few minutes after plasma treatment, is characterized by depositing distilled water drops of 2 μl volume using a Krüss Easy Drop contact angle measurement system. Droplets are placed at different positions on the PCL samples and images are captured a few seconds after deposition of each drop. Based on the imaged water drop profile, the static water contact angle value is obtained using Laplace-Young
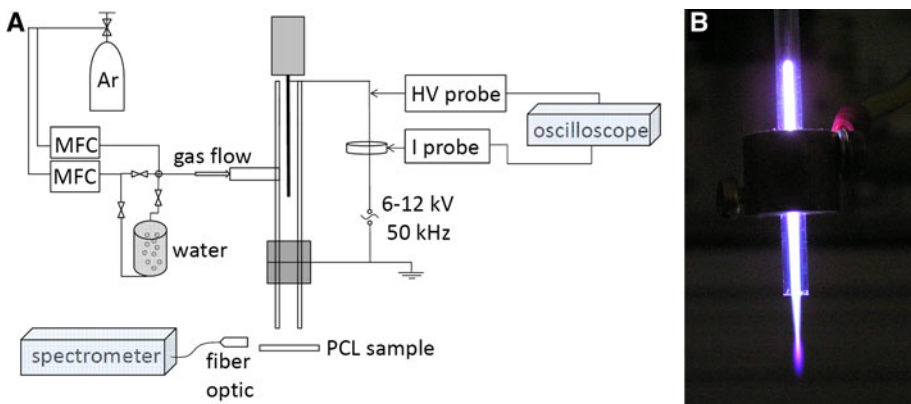

Fig. 2 Experimental set-up (**a**) and visual view (**b**) of the plasma jet

curve fitting. Every reported contact angle value in this work is the average of 5 independent measurements and standard deviations vary from 0.3° to 2.0°.

X-ray Photoelectron Spectroscopy

Besides contact angle measurements, PCL samples are also studied by XPS to obtain the elemental composition and to get an insight in the chemical functions introduced on the surface by plasma treatment. XPS measurements are performed on an ESCA S-probe VG monochromatized spectrometer equipped with an Al K_α X-ray source (hν = 1,486 eV). The pass energy for survey spectra, recorded over the energy range 0–800 eV was 157 eV with 1 eV step size and for high-resolution C1s spectra 56 eV with 0.06 eV step size. The base pressure in the main chamber during analyses is not higher than 5×10^{-8} Pa, the spot size is kept constant at 0.5 mm $\times$ 1 mm and the spectra are acquired at an emission angle of 45°. A nickel grid was applied as well as charge neutralization with 4 eV in order to avoid charging effects. Elements present on the surface are identified from survey spectra and quantified [in atomic % (at%)] with CasaXPS software using a linear background and applying the relative sensitivity factors supplied by the manufacturer of the instrument. CasaXPS software is also used for the curve fitting of the high-resolution C1s peaks: the hydrocarbon component of the C1s spectrum (285.0 eV) is used to calibrate the energy scale and a Shirley background is chosen. After this calibration step, the C1s peaks are deconvoluted using Gaussian–Lorentzian peak shapes with a 30 % Lorentzian component and the full-width at half maximum (FWHM) of each line shape is constrained below 1.6 eV.

Results

Optical Characterization of the Discharge

The chemical species present in the plasma jet can be identified by optical emission spectroscopy (OES) and Fig. 3 shows the emission spectra observed in different argon/water vapour mixtures. The most intensive argon lines can be found in the spectral region between 680 and 900 nm, which can be assigned to different excited states of the argon atom [34]. The discharge also produces a significant amount of UV radiation, which belongs to transitions of the OH band at 308 and 287 nm [35]. Apart from the previously mentioned lines, spectral lines from atomic oxygen (777 and 844 nm) and nitrogen (310–440 nm) can be identified. In pure argon, these lines result from dissociation and ionization of the surrounding atmosphere which contains nitrogen, oxygen and water while in the argon/water vapour mixtures, they can also result from the water vapour present in the feed gas. As seen in Fig. 3, an increase in water content results in a decrease of most spectral line intensities and Fig. 4 shows the normalized intensity (I_{Ar+H2O}/I_{Ar}) of the most pronounced spectral lines as a function of water vapour content. One can observe in Fig. 4 that the emission of argon lines (696, 763 and 801 nm) and the atomic oxygen emission (777 nm) decrease as a function of water vapour content. These decreases can be explained by a decrease in electron temperature at elevated water vapour contents: the addition of molecular species to a discharge in noble gases results in an increasing energy transfer between electrons and heavy species (such as H_2O) causing a reduction in electron temperature [35]. Figure 4 also shows that a maximum in the OH emission intensity (OH (A) ➔ OH (X)) is observed for the argon/water vapour mixture with 0.05 % of water
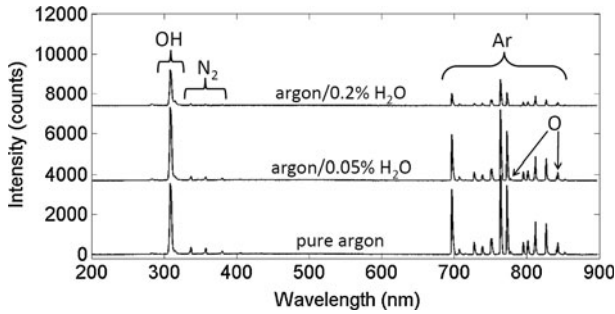
Fig. 3 Axial optical emission spectra of the plasma jet in argon and argon/water vapour mixtures (total gas flow: 2.0 slm, discharge power: 7.9 W)

vapour due to the very effective dissociative excitation of water with argon metastables (H_2O + Ar* ➜ Ar + OH (A) + H) [33]. A larger water vapour content however results in a drastic decrease in OH emission intensity. This behaviour at high water vapour contents has been previously explained in literature by Nikiforov et al. [33]: a higher water content leads to a more pronounced quenching of the radiative OH (A) species (OH (A) + H_2O ➜ OH (X) + H_2O).

Plasma Modification of PCL with an APPJ Sustained in Argon

In this results section, plasma surface modification of PCL is performed with an APPJ sustained in pure argon and the influence of different operating parameters is examined in detail. A first parameter that influences the effect of the plasma jet treatment is the plasma exposure time, which can be altered by changing the plasma scanning velocity. The treatment time τ can be obtained by dividing the active diameter of the jet (= 1.3 mm) to the plasma scanning velocity. Figure 5 depicts the evolution of the water contact angle on the plasma-treated PCL samples as a function of plasma exposure time. The distance between the edge of the capillary and the PCL sample is kept constant at 4 mm, while the discharge power and argon flow rate are maintained at 4.1 W and 2.0 slm, respectively.
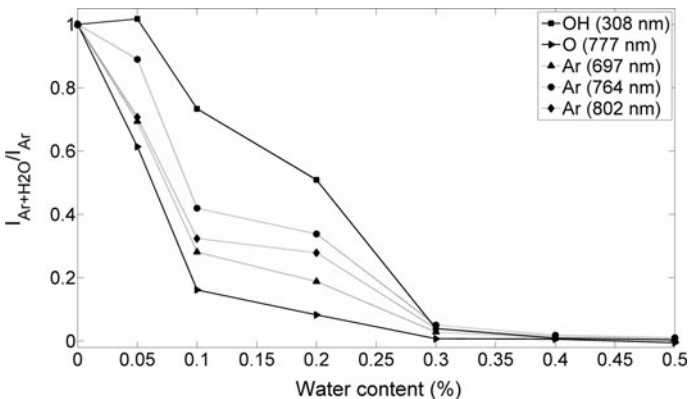

Fig. 4 Normalized peak emission intensity of different excited species as a function of water content in the plasma jet (discharge power: 7.9 W, total gas flow: 2.0 slm)
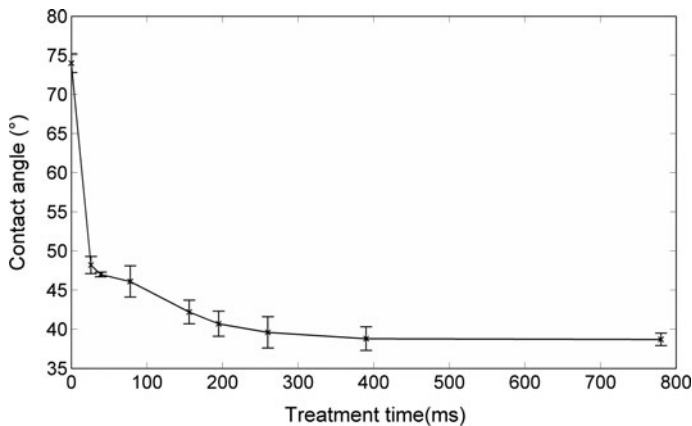
Fig. 5 Water contact angle as a function of plasma treatment time for PCL samples plasma-treated in pure argon (discharge power: 4.1 W, argon flow: 2.0 slm)

The water contact angle of the untreated PCL film is 74° and gradually decreases to 38° with increasing plasma treatment time. However, when the PCL samples are plasma-treated for more than 390 ms, the contact angle remains unchanged, showing that there is a saturation of the plasma effect on the PCL surface. The large diminution of the contact angle after plasma treatment however demonstrates the strongly increased wettability, suggesting that the plasma-treated PCL surfaces contain a large amount of hydrophilic groups [36–39]. To proof this statement, XPS measurements are performed on an untreated and a plasma-treated PCL sample (treatment time: 390 ms). Based on the XPS survey scans, the atomic compositions of the polymer samples are determined and the results are shown in Table 1. This table indicates that after argon plasma treatment, the oxygen content increases from 23 to 29 at%. The plasma treatment also introduces a very small amount of nitrogen, however, this nitrogen incorporation is negligible compared to the oxygen inclusion. To determine which chemical groups are present on the surface of the untreated and plasma-treated PCL samples, curve-fitting of high-resolution C1s peaks is also performed and the results are presented in Fig. 6. The C1s envelope of the untreated PCL sample can be decomposed into 3 distinct peaks: a peak at 285.0 ± 0.1 eV corresponding to C–C and C–H bonds, a peak at 286.5 ± 0.1 eV due to C–O functional groups and a peak at 289.1 ± 0.1 eV, which can be attributed to O–C=O groups [40]. As shown in Fig. 6, changes in the C1s peak can be observed after argon plasma treatment: the peak at 285.0 eV slightly decreases while the peaks at 286.5 and 289.1 eV increase. Moreover, a new peak at 287.7 ± 0.1 eV, which can be attributed to C=O groups appears after plasma treatment. Based on the deconvoluted C1s peaks, the concentration of the different chemical bonds can be calculated and the obtained results are given in Table 1. This table clearly shows that the concentration of C–C and/or C–H bonds decreases after argon plasma treatment, while the concentration of oxygen-containing groups (C–O, C=O and O–C=O) strongly increases. The primary effect of the argon plasma jet on the polymer surface is most likely the hydrogen abstraction by oxygen atoms and OH radicals present in the discharge [41]. However, cleavage of the C–C polymer backbone is also possible [41]. The created polymer radicals will subsequently react with atomic oxygen, molecular oxygen, ozone and OH radicals leading to the implantation of oxygen-containing groups on the polymer surface [41].

Table 1 Atomic composition and concentration of chemical groups on an untreated and plasma-treated PCL sample (argon jet, treatment time: 390 ms, discharge power: 4.1 W, argon flow rate: 2.0 slm, capillary edge-polymer distance: 4 mm)

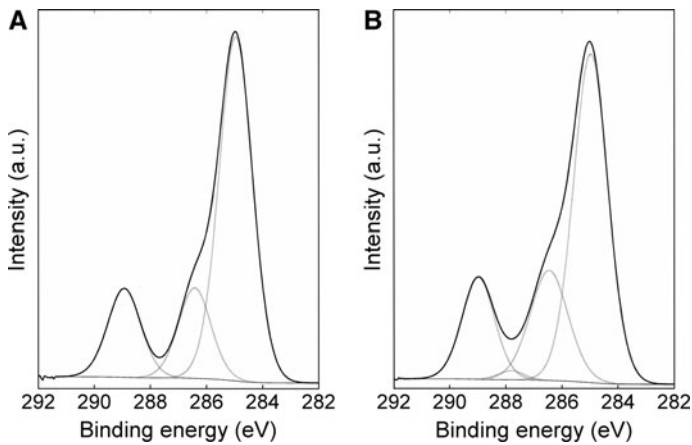| Sample	C (at%)	O (at%)	N (at%)	C–C/C–H (%)	C–O (%)	O–C=O (%)	C=O (%)
Untreated	77	23	0	66	17	17	0
Plasma-treated	70	29	1	59	22	18	1

Fig. 6 High-resolution C1s peak of **a** an untreated PCL sample and **b** an argon plasma-treated PCL sample (discharge power: 4.1 W, argon flow: 2.0 slm, treatment time: 390 ms, capillary edge-polymer distance: 4 mm)

Besides plasma treatment time, also the distance between the edge of the capillary and the polymer surface will influence the efficiency of the plasma jet. Table 2 presents the PCL water contact angle for varying capillary edge-surface distances, while the discharge power, argon flow and plasma treatment time are kept constant at 4.1 W, 2 slm and 78 ms, respectively. Table 2 clearly shows that the contact angle decrease is less pronounced when the distance between the capillary edge and the sample is increased. Due to the limited lifetime of the reactive plasma species responsible for oxygen incorporation, only a low amount of these active species will reach the polymer surface at high capillary-sample distances, resulting into less hydrophilic surfaces. Therefore, one can conclude that the position of the PCL surface should be as close as possible to the capillary edge in order to obtain the most efficient decrease in water contact angle. For an easy operation of the plasma jet, the capillary-edge sample distance will however be kept constant at 4 mm for all subsequent measurements performed in this work.

Table 2 PCL water contact angle values for varying capillary edge-PCL surface distances (discharge power: 4.1 W, argon flow: 2 slm, plasma treatment time: 78 ms)

Plasma-sample distance (mm)	1.0	2.0	4.0	6.1	8.0	10.0	12.3	15.0	20.4	29.6	40.3
Water contact angle (°)	44.7	45.3	46.1	48.6	49.9	51.1	55.1	59.6	63.8	65.1	65.1

Besides plasma-polymer distance and treatment time, also discharge power and argon flow rate can affect the surface modification process, as shown in Table 3 (plasma treatment time: 78 ms). These results show that with increasing argon flow rate, the water contact angle gradually decreases to a minimal value (43°) at 2.5 slm. At an even higher argon flow rate (3.0 slm), the water contact angle remains at approximately 43°. Increasing the argon flow rate results in a higher flux of reactive oxygen species reaching the polymer surface, leading to a more pronounced surface modification effect. Table 3 also shows that the water contact angle value gradually decreases with increasing discharge power. An increasing discharge power results in the presence of a higher amount of reactive oxygen species and thus a more effective surface modification process.

Plasma Modification of PCL with an APPJ Sustained in Argon/Water Vapour Mixtures

In this section, it is investigated whether it is possible to increase the polymer modification efficiency by adding a small amount of water vapour to the argon plasma jet. For that reason, plasma surface modification of PCL is performed in different argon/water vapour mixtures at similar operating conditions (discharge power: 7.9 W, treatment time: 78 ms, total gas flow: 2.0 slm, capillary edge-polymer distance: 4 mm). Table 4 shows the PCL water contact angle as a function of water vapour content. This table shows that the water contact angle of the plasma-treated PCL surfaces reaches a minimal value (45.3°) at 0.05 % of water vapour, while a further increase in water vapour content results in a less effective treatment of the PCL surface with a contact angle value of 49.1° at the highest water vapour concentration (0.5 %). The influence of water vapour content on the chemical composition of the PCL samples is also investigated using XPS and the results are also shown in Table 4. The highest oxygen inclusion can be found when 0.05 % of water vapour is added to the argon feeding gas. This conclusion can be correlated with the previously presented optical emission spectroscopy results (Fig. 4). By observing the emission intensity of OH (A–X) at 308 nm, one can gather information on the electronically excited state OH (A) in the plasma jet and it was found that a maximum amount of OH (A) radicals was found at a water vapour content of 0.05 %. However, not the excited state OH (A) is responsible for surface modification, but the electronic ground state OH (X). Measurements of the number density of OH (X) radicals in an atmospheric pressure plasma jet can however be carried out using ultraviolet absorption spectroscopy, as shown by Hong et al. [42]. These authors experimentally proved that the maximum density of OH (X) radicals is found at the maximum OH emission intensity. Therefore, one can conclude that at a water vapour content of 0.05 %, a maximum amount of OH (X) radicals is present in the plasma jet, which can in turn explain the highest oxygen incorporation at this water vapour content. By optimizing the OH (X) radical yield in the plasma jet, the best polymer modification efficiency can thus be obtained.

Table 3 PCL contact angle values for different argon flow rates and discharge powers (treatment time: 78 ms)

Argon flow (slm)	0.5	1.0	1.5	2.0	2.5	3.0	2.0					
Power (W)	4.1							5.5	6.5	7.9	9.5	11.5	13.0
Contact angle (°)	67.1	55.0	48.4	46.1	43.0	43.4	45.6	44.6	44.0	43.5	42.3	40.8

Table 4 Contact angle value, atomic composition and concentration of chemical groups on PCL samples plasma-treated in different argon/water vapour mixtures (discharge power: 7.8 W, treatment time: 78 ms, capillary edge-sample distance: 4 mm)

Water vapour content (%)	Contact angle (°)	C (at %)	O (at %)	N (at %)	C–C/ C–H (%)	C–O (%)	O–C=O (%)	C=O (%)
0.0	46.1	71	28	1	62	20	17	1
0.05	45.3	70	29	1	59	22	18	1
0.1	46.5	71	28	1	62	20	17	1
0.2	46.7	72	27	1	64	19	16	1
0.4	48.1	72	27	1	65	18	16	1
0.5	49.1	73	26	1	66	18	15	1

Conclusion

In this work, the chemical species present in an atmospheric pressure plasma jet in argon and argon/water vapour mixtures have been determined using optical emission spectroscopy. It has been found that the emission intensity of OH radicals (OH (A) ➜ OH (X)) can be altered by adding water vapour to the argon working gas: the maximal OH emission intensity can be obtained in an argon/0.05 % water vapour mixture. In a second part of the work, the plasma jet has been successfully employed for the surface modification of PCL samples. From contact angle and XPS measurements, it was found that the plasma jet can significantly increase the hydrophilicity of PCL by incorporating oxygen-containing groups (C–O, C=O and O–C=O). At similar operating conditions, the most efficient oxygen incorporation was however found after plasma treatments in argon/0.05 % water vapour mixtures. This could be attributed to the high OH (X) concentration in this gas mixture. Therefore, the OH (X) radical yield in the discharge should be optimized to obtain a high polymer modification efficiency. The performed plasma treatments can have a significant positive effect on cell adhesion and proliferation, thereby opening possibilities to many interesting biomedical applications.

References

1. Langer R, Vacanti JP (1993) Science 260:920–926
2. Wang YJ, Lu L, Zheng YD, Chen XF (2006) J Biomed Mater Res A 76A:589–595
3. Djordjevic I, Britcher LG, Kumar S (2008) Appl Surf Sci 254:1929–1935
4. Desmet T, Morent R, De Geyter N, Leys C, Schacht E, Dubruel P (2009) Biomacromolecules 10:2351–2378
5. Ryu GH, Yang WS, Roh HW, Lee IS, Kim JK, Lee GH, Lee DH, Park BJ, Lee MS, Park JC (2005) Surf Coat Technol 193:60–64
6. Hutmacher DW (2000) Biomaterials 21:2529–2543
7. Chen GP, Ushida T, Tateishi T (2002) Macromol Biosci 2:67–77
8. Morent R, De Geyter N, Desmet T, Dubruel P, Leys C (2011) Plasma Process Polym 8:171–190
9. Shen H, Hu XX, Yang F, Bel JZ, Wang SG (2007) Biomaterials 28:4219–4230
10. Morent R, De Geyter N, Trentesaux M, Gengembre L, Dubruel P, Leys C, Payen E (2010) Plasma Chem Plasma Process 30:525–536
11. Park GE, Pattison MA, Park K, Webster TJ (2005) Biomaterials 26:3075–3082
12. Zhu YB, Gao CY, Liu XY, Shen JC (2002) Biomacromolecules 3:1312–1319
13. Chong MSK, Lee CN, Teoh SH (2007) Mat Sci Eng C 27:309–312
14. Ho MH, Lee JJ, Fan SC, Wang DM, Hou LT, Hsieh HJ, Lai JY (2007) Macromol Biosci 7:467–474

15. Montanari L, Costantini M, Signoretti EC, Valvo L, Santucci M, Bartolomei M, Fattibene P, Onori S, Faucitano A, Conti B, Genta I (1998) J Controlled Release 56:219–229
16. Place ES, George JH, Williams CK, Stevens MM (2009) Chem Soc Rev 38:1139–1151
17. Ho MH, Hou LT, Tu CY, Hsieh HJ, Lai JY, Chen WJ, Wang DM (2006) Macromol Biosci 6:90–98
18. Cheng ZY, Teoh SH (2004) Biomaterials 25:1991–2001
19. Borcia G, Brown NMD (2007) J Phys D-Appl Phys 40:1927–1936
20. Heyse P, Dams R, Paulussen S, Houthofd K, Janssen K, Jacobs PA, Sels BF (2007) Plasma Process Polym 4:145–157
21. Martin S, Massines F, Gherardi N, Jimenez C (2004) Surf Coat Technol 177:693–698
22. Han I, Kwon BJ, Vagaska B, Kim BJ, Kang JK, Lee MH, Kim HH, Park JC, Wang KK, Kim YR, An JS, Lee JM, Hyun CY, Jeong JH, Lim SJ (2011) Macromol Res 19:1134–1141
23. Park SA, Lee SH, Kim W, Han I, Park JC (2011) J Tissue Eng Regen Med 8:A23–A27
24. Little U, Buchanan F, Harkin-Jones E, Graham B, Fox B, Boyd A, Meenan B, Dickson G (2009) Acta Biomater 5:2025–2032
25. Yildirim ED, Gandhi M, Fridman A, Guceri S, Sun W (2008) In: Guceri S, Fridman A (eds) Plasma assisted decontamination of biological and chemical agents. Springer, Dordrecht
26. Martins A, Pinho ED, Faria S, Pashkuleva I, Marques AP, Reis RL, Neves NM (2009) Small 5:1195–1206
27. Lommatzsch U, Pasedag D, Baalmann A, Ellinghorst G, Wagner HE (2007) Plasma Process Polym 4: S1041–S1045
28. Schutze A, Jeong JY, Babayan SE, Park J, Selwyn GS, Hicks RF (1998) IEEE Trans Plasma Sci 26:1685–1694
29. Weltmann KD, Kindel E, Brandenburg R, Meyer C, Bussiahn R, Wilke C, von Woedtke T (2009) Contrib Plasma Phys 49:631–640
30. Weltmann KD, Brandenburg R, von Woedtke T, Ehlbeck J, Foest R, Stieber M, Kindel E (2008) J Phys D-Appl Phys 41:194008
31. Hibert C, Gaurand I, Motret O, Pouvesle JM (1999) J Appl Phys 85:7070–7075
32. Massines F, Gouda G (1998) J Phys D-Appl Phys 31:3411–3420
33. Nikiforov AY, Sarani A, Leys C (2011) Plasma Sources Sci Technol 20:015014
34. Bornholdt S, Wolter M, Kersten H (2010) Eur Phys J D 60:653–660
35. Sarani A, Nikiforov AY, Leys C (2010) Phys Plasmas 17:063504
36. Morent R, De Geyter N, Leys C (2008) Nucl Instrum Methods Phys Res B 266:3081–3085
37. Morent R, De Geyter N, Leys C, Gengembre L, Payen E (2008) Surf Interface Anal 40:597–600
38. De Geyter N, Morent R, Leys C (2008) Surf Interface Anal 40:608–611
39. Morent R, De Geyter N, Gengembre L, Leys C, Payen E, Van Vlierberghe S, Schacht E (2008) Eur Phys J Appl Phys 43:289–294
40. Briggs D (1998) Surface analysis of polymers by XPS and static SIMS. Cambridge University Press, Cambridge
41. Dorai R, Kushner MJ (2003) J Phys D-Appl Phys 36:666–685
42. Hong YJ, Nam CJ, Song KB, Cho GS, Uhm HS, Choi DI, Choi EH (2012) J Instrum 7:C03046